Slug flow in horizontal pipes with transpiration at the wall

2011 J. Phys.: Conf. Ser. 318 022014

(http://iopscience.iop.org/1742-6596/318/2/022014)

Slug flow in horizontal pipes with transpiration at the wall

J. B. R. Loureiro & A. P. Silva Freire

Mechanical Engineering Program, Federal University of Rio de Janeiro (COPPE/UFRJ), C.P. 68503, 21.941-972, Rio de Janeiro, RJ, Brazil.

E-mail: jbrloureiro@mecanica.ufrj.br

Abstract. The present work investigates the behaviour of slug flows in horizontal pipes with a permeable wall. Measurements of pressure drop and of local velocity are given for nine different flow conditions. The liquid phase velocity was measured with laser Doppler anemometry. Single-phase data are compared with the results of other authors. The influence of flow transpiration and of roughness on the features of slug flows is shown to be pronounced. A Shadow Sizer system coupled with Particle Image Velocimetry is used to account for the properties of the slug cell.

1. Introduction

Horizontal drilling technology has achieved a great degree of success in the last twenty years. The large improvements in the technique have meant that horizontal bore hole lengths with more than 2,500 meters can be easily found. The aim of a horizontal well is to expose significant areas of reservoir rock to the well bore surface. To fill the space between the screen casing and the bore hole, a high conductivity hydraulic sand or gravel packed "wall" is normally used. Upon the action of the reservoir large pressures, fluid is then transpired from the rock reservoir into the well bore. Over short lengths, the effects of transpiration on the flow properties including the pressure drop can be neglected. However, over long ranges the skin-friction needs to be detailed known so that realistic estimates of pressure drop can be made.

For fully developed laminar flow of an incompressible viscous fluid in a porous pipe with suction or injection, exact solutions of the Navier-Stokes equations can be found (see, e.g., the recent work of Oxarango et al. 2004 and Erdogan & Imrak 2005 or the classical works of Berman 1953, Terrill 1964 and Bundy & Weissberg 1970). These flows are typical of filtration systems and, therefore, have been studied intensively mainly by the chemical engineering community.

In petroleum applications, however, most industrial flows occur at very large Reynolds number so that turbulent effects must be taken into account. The immediate consequence is that any proposed solution must be followed by a representative closure hypothesis and by boundary conditions that account for wall roughness. The evident increase in complexity means that approximate solutions must be sought through analytical methods. In fact, an application of perturbation techniques to the Reynolds Averaged Navier-Stokes equations (RANS) together with the mixing-length hypothesis (Stevenson 1963, Simpson 1967, Silva Freire 1988) yields a local analytical solution that is valid in the fully turbulent region and has an explicit dependence

on the transpiration rate. An integration of this solution can be made to yield a resistance law for smooth and rough pipes at large Reynolds numbers that contains a bi-logarithmic term. The bi-logarithmic law naturally incorporates the effects of local Reynolds number and transpiration rate.

The underlying assumption of this method is that flow transpiration at the wall is homogeneous. This approach is different from other authors (see, e.g., the review paper of Clemo 2006), who instead have preferred to describe frictional losses in perforated pipes through a decomposition of effects: wall friction, perforation friction and mixing effects. In most cases, perforation friction is associated with an increase in roughness. The mixing effects, on the other hand, are compared to the problem of multiple interacting jets in a cross flow. This solution strategy results in such a complex analysis that only external empirical evidence can be used to determine the correct behavior of the friction contribution.

On the other hand, in many important applications the flows of interest include long isolated bubbles, such as those observed in horizontal slug flows. To the best of the present authors' knowledge, this particular problem has not been addressed before: slug flow in pipes with wall transpiration.

The purpose of the present work is to carry out an experimental study of single-phase and slug flow in horizontal pipes with a permeable wall. In addition to pressure loss data, the work presents local velocity and turbulent profiles obtained through Laser-Doppler Anemometry. The analysis also compares single-phase data with the measurements of Olson & Eckert 1966 and of Su & Gudmunsson 1998 and with results obtained with the theory of Cruz et al. 2009. Local mean velocity measurements are made to assess the bi-logarithmic term predicted by Silva Freire 1988.

Pressure drop data are used to assess the differences between predictions given by the single-phase model and the slug flow. The influence of flow transpiration and of roughness on the features of the slug is accounted for by Laser-Doppler measurements in two test sections. A Shadow Sizer system coupled with a Particle Image Velocimetry system is used to account for the properties of the slug cell.

2. Theoretical background

2.1. Resistance law for smooth pipes
The friction coefficient λ can be defined by

$$(p_1 - p_2)L^{-1} = (\lambda D^{-1})(2^{-1}\rho)U_m^2, \tag{1}$$

where D denotes the pipe diameter, U_m is the mean flow velocity and L the length of a fluid cylinder.

For very large Reynolds numbers, the velocity distribution in the near wall fully turbulent region is given by

$$uu_*^{-1} = \varkappa^{-1} \ln\left(yu_*\nu^{-1}\right) + A, \tag{2}$$

where y is the wall distance, u_* is the friction velocity ($=\sqrt{\tau_w/\rho}$), $\varkappa$ ($= 0.4$) is von Karman's constant and $A = 5.5$.

An integration of Eq. (2) over the cross-sectional area of a pipe together with some algebraic manipulations gives the resistance law for smooth pipes,

$$(\sqrt{\lambda})^{-1} = 2.035 \log\left(R_e\sqrt{\lambda}\right) - 0.8, \tag{3}$$

with $R_e = U_m D\nu^{-1}$.

2.2. Resistance law for smooth pipes with wall transpiration

For flow subject to wall transpiration, Eq. (3) is clearly not valid anymore. The result of the injection or suction of fluid into an oncoming flow is to modify the velocity distribution throughout the boundary layer so that drag is either reduced or increased. Any expression advanced with the purpose of determining the friction coefficient should therefore reflect this. Furthermore, an explicit dependence of Eq. (3) on the transpiration rate should be expected.

In Silva Freire 1988 the matched asymptotic expansions method was applied to the equations of motion to find a law of the wall in which the additive parameter A varied with transpiration. The resulting expression is

$$u^+ = \varkappa^{-1}\ln\left(y^+\right) + A + \Pi\varkappa^{-1}W\left(y\delta^{-1}\right) + v_w^+\left((2\varkappa)^{-1}\ln\left(y^+\right) + 2^{-1}A\right)^2 + \tilde{\Pi}\varkappa^{-1}W\left(y\delta^{-1}\right), \quad (4)$$

with $u^+ = uu_*^{-1}$, $y^+ = yu_*\nu^{-1}$, $v_w^+ = v_w u_*^{-1}$, v_w = normal velocity at the wall and A is given by:

$$A = 5 - 512(v_w U^{-1}), \quad (5)$$

and parameters Π and $\tilde{\Pi}$ and function W are related to the universal wake function.

An integration of Eq. (4) over the cross-sectional area of a pipe, gives

$$U_m = U - 3.75u_* - v_w(1.86A + 2.34\ln {Re^+}^2 - 5.47), \quad (6)$$

with $Re^+ = Ru_*\nu^{-1}$.

Some further algebraic manipulations with

$$U_m {u_*}^{-1} = 2\sqrt{2}(\sqrt{\lambda})^{-1}, \quad (7)$$

give

$$\begin{aligned} 1 = {} & \sqrt{\lambda}(2\sqrt{2})^{-1}(2,5\ln(Re^+) + A - 3,75) \\ & + v_w^+(1,56\ln^2(Re^+) + (1,25A - 4,68)\ln(Re^+) + 4^{-1}A^2 + 1,86A + 5,47), \end{aligned} \quad (8)$$

where

$$v_w^+ = v_w {U_m}^{-1} \qquad \text{and} \qquad Re^+ = (U_m D\nu^{-1})(4\sqrt{2}^{-1}\sqrt{\lambda}). \quad (9)$$

The transcendental equation, Eq. (8), gives λ for given Re^+ and v_w^+.

2.3. Resistance law for rough pipes

The law of resistance for flow in a rough pipe was shown by Nikuradse 1933 to have the form

$$u{u_*}^{-1} = \varkappa^{-1}\ln\left(y{k_s}^{-1}\right) + B, \quad (10)$$

where k_s is a characteristic length of the roughness and B = 8.5 (completely rough regime).

In fact, B was shown to be a function of Re_k ($= k_s u_*\nu^{-1}$). The behaviour of B for the three types of flow regime discussed by Nikuradse 1933 has been studied by several authors. For example, Ligrani & Moffat 1986 suggest the following functional dependence

$$B = 8.5\sigma + (1-\sigma)\varkappa^{-1}\ln(Re_k) + (1-\sigma)C, \quad (11)$$

where $Re_k = k_s u_*/\nu$, $C = 5.1$ and $\sigma = \sin((1/2)\pi g)$ with

$$g = \ln\left(Re_k Re_{k,s}^{-1}\right)\left(\ln\left(Re_{k,r} Re_{k,s}^{-1}\right)\right)^{-1}, \tag{12}$$

$Re_{k,s} = 5$, $Re_{k,r} = 70$ and this approximation is valid in $5 \leq Re_k \leq 70$.

The resistance formula for flow in a rough pipe can be obtained by integrating Eq. (10) over the cross-sectional area of a pipe. The result is

$$\lambda = [0.88 \ln(Rk_s^{-1}) + 0.35B - 1.33]^{-2}. \tag{13}$$

A comparison of Eq. (13) with the experiments of Nikuradse shows that for a fully rough regime the ln additive term should be replaced by 1.74.

2.4. Resistance law for rough pipes with wall transpiration

A law of resistance for rough pipes with wall transpiration can now be deduced provided the results of the previous sections are taken into account. Let us define $Re^+ = R/k_s$ and $A_k = B$ - 512 v_w/U. It follows immediately from Eqs. (8) and (13) that

$$\begin{aligned} 1 = \sqrt{\lambda}(2\sqrt{2})^{-1}(2.5 \ln(Rk_s^{-1}) + A_k - 3.75) + v_w^+(1.56 \ln^2(Rk_s^{-1}) \\ + (1.25A_k - 4.68) \ln(Rk_s^{-1}) + 4 - 1A_k^2 + 1.86A_k + 5.47). \end{aligned} \tag{14}$$

3. Experiments

The main objective of the experiments was to study the influence of flow transpiration on the distribution of pressure loss in turbulent flows inside rough, porous circular pipes. The investigation was carried out for single phase flows (water) as well as for two-phase air-water slug flows. To the present authors' knowledge, this is the first time that such experiments are performed.

3.1. Experimental set up

To simulate flow transpiration from a rock reservoir to a horizontal well, a test bench was built in the Flow Measurement Laboratory of the Brazilian Institute of Standards (INMETRO). The test section consists of three concentric stainless-steel tubes, as shown in Figure 1. The inner pipe was made by winding on a cylindrical mandrel four layers of a very fine wire mesh that were subsequently welded at the joint points to produce a rigid 34 mm diameter tube. Using the same construction method, an intermediate tube with 95 mm diameter was made of a single perforated sheet 1.5 mm thick and 50 percent porosity. The annular region between the inner and intermediate pipes was filled with small bits (2.5 mm external diameter, 0.5 internal diameter, 3.0 mm length) to simulate the porosity of a rock reservoir. The outer pipe consisted of a solid 3 mm thick, 123 mm diameter stainless-steel tube. The room between the intermediate and outer pipes served as a plenum chamber, so as to guarantee that an uniform transpiration rate could be achieved for every test condition.

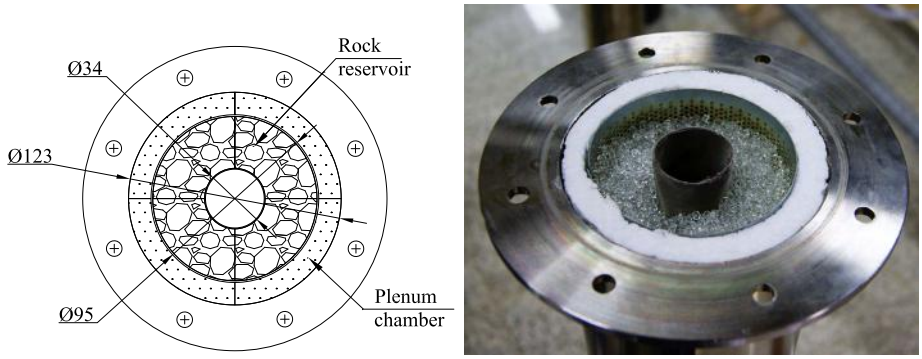

Figure 1. Description of the test section: a) schematic view, b) general illustration.

A schematic diagram of the piping system is shown in Figure 2. The piping system consisted of two water circulation loops. The first loop was used to supply water and air to the through flow in the porous, rough pipe. Water for transpiration was introduced through an injection valve into the plenum chambers. The whole apparatus consisted of six 1-m segments. These segments were connected together through 25-mm thick sheets of plexiglass that served as inspection windows. The windows allowed the use of optically based measurement instruments. Thus, the total length of the test section was 6175 mm. A Netzsch progressive cavity pump was used to provide the water supply. The system was configured so that a variety of different flow rates in the main line and in the through flow could be achieved. The air nozzle was installed 1-m upstream of the well entrance. The connection pipe between the air nozzle and the entrance was made of plexiglass so that flow visualization was permitted.

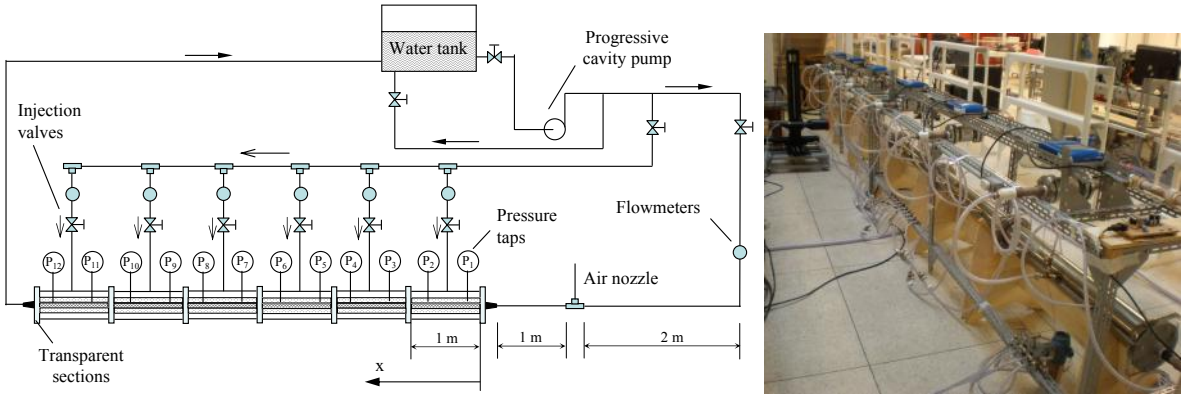

Figure 2. Overview of the experimental set up: a) schematic diagram, b) general view.

3.2. Measurements of flow properties

Every 1-m of test section was fitted with two pressure taps with 50-mm spacing between them. A set of valves connected the taps to a differential pressure transducer (Emerson 3051) to provide the pressure distribution along the whole length of the simulated well. Every water supply line was fitted with a flowmeter. All velocity profiles and additional flow rates were measured with laser-Doppler anemometry. The one-component Dantec laser-Doppler anemometry system used a 400 mW Ar-ion tube laser and was operated in the forward-scatter mode to measure mean and fluctuating velocity fields. A Bragg cell unit was used to introduce a digitally-controlled electronic shift in order to resolve the direction of the flow field and give correct measurements of near-zero mean velocities. The two light beams that emerged from the 60 mm diameter FiberFlow probe were made to pass through a beam expander with expansion ratio of 1.98. This optical component was used to increase the beam spacing and, as a consequence, to provide a

smaller measurement volume of dimensions 49.6 μm x 49.9 μm x 150 μm. Front lens with 310 mm focus length were mounted on the probe to accurately position the measurement volume on the centerline of the inner pipe. The signals from the photo-multipliers were digitized and processed through a burst spectrum analyzer BSA P60 operating in single measurement per burst mode. The Dantec BSA Flow Software 4.50 was used to calculate the Doppler frequencies and the resulting velocity samples. A series of LDA biases were avoided by adjusting the strictest parameters on the data processor and software.

The PIV measurements were performed with a two-dimensional La Vision system. The light source was furnished by a double pulsed Nd:YAG laser that produced short duration (10 ns) high energy (120 mJ) pulses of green light (532 nm). The collimated laser beam was transmitted through a cylindrical (15 mm) and a spherical (500 mm) lens to generate a 1 mm thick light sheet. The reflected light was recorded at 15 Hz by a CCD camera with 1280 x 1024 pixels and 12-bit resolution. The camera was fitted with a Nikkor 105 mm f/2.8D lens. Image calibration was made by taking pictures of a reference target specially designed for the present purpose.

For all the measurements, computational conditions for the velocity vectors were fixed. Adaptive correlation (DaVis 7.1 Software) has been processed on 32x32 pixels-size final interrogation windows, with 50% overlap, which gives 64x64 vectors. The pixel resolution is 6.45x6.45 μm. Particle image treatment using subpixel cell shifting and deformation, allowing bias and random error reduction. A widely accepted estimation of the absolute displacement error using these algorithms is 0.05 pixels. Different thresholds including signal-to-noise ratio and velocity vector magnitude were used as post-processing steps.

Since the majority of classifications for two-phase flow patterns are based on the visual inspection of the flow, it is highly important to have an accurate imaging procedure for turbulent pipe flows. The present work used the Shadow Sizer (Dantec Dynamics) to quantify the properties of the air-water flow on the well set up. This system is comprised of a high speed camera (NanoSense MK III) and a constellation led back light that provided high resolution images (1289 x 1024 pixels) at 2000 Hz frame rate. The software Dynamic Studio is responsible for triggering the camera and the illumination system, as well as detecting contour differences on the images to provide statistical results about the flow. However, since the code is not fitted for quantifying slug flows, a special software was implemented in Mathematica for the calculation the quantities of interest.

4. Results

The general flow conditions are shown in Table 1. Nine experiments in all were performed. For the slug flows, the liquid flow rate was 0.3 ls^{-1}; the gas flow rate was 0.6 ls^{-1}.

Table 1. Experimental flow conditions.

Flow	U_{max} $[ms^{-1}]$	v_w^+	Measured quantity
single flow	0.5	0.0	U (velocity), P (pressure)
single flow	0.75	0.0	U, P
single flow	1	0.0	U, P
single flow	1.88	0.0	U, P
slug flow	0.5	0.0	U, P
single flow	1.91	0.006	U, P
single flow	2.42	0.008	U, P
slug flow	0.5	0.006	U, P
slug flow	0.5	0.008	U, P

4.1. Single phase flow

Single phase flow experiments must be performed so that the roughness length, k_s, can be determined. For the sake of comparison, the present results are compared with the data of Olson & Eckert 1966 and of Su & Gudmunsson 1998.

To study the effects of flow injection on the thermal protection of walls, these authors analyzed the turbulent flow of air in a porous tube with circular cross section. The tube had a 50 percent porosity, having been wrapped with several layers of rayon cloth to ensure uniform injection rates. The data reduction was based on a balance of the mass and momentum equations. Results were given for the local mean velocity profiles, static pressure, mass flow rate and wall shear stress.

Su & Gudmunsson 1998 divided the total pressure drop in horizontal pipes into four distinct effects: flow acceleration, wall friction, perforation roughness and fluid mixing. Their work suggests that the pressure drop due to the roughness provoked by the perforation is eliminated by the inflow when the transpiration rate reaches a certain limit. Experiments were conducted in a pipe with 0.022 mm internal diameter and 0.6 m length. The perforation was provided by drilling 158 holes of 3 mm in the pipe. The resulting porosity was 0.027. The measured pressure drop due to wall friction, perforation roughness and mixing effects was obtained by subtracting the pressure drop due to flow acceleration from the total pressure drop. The ordinary wall frictional pressure drop was calculated through the Darcy-Weisbach equation.

From the above description, it is clear that the homogeneous wall transpiration condition preconceived by Eq. (14) is much more likely to be satisfied by the data of Olson and Eckert (1966). The very low porosity of Su & Gudmunsson 1998, in principle, does not characterize a uniform wall condition. It is also very clear that the present flow configuration is similar to that of Olson & Eckert 1966.

Various experiments with Reynolds number varying from 30.000 to 60.000 were performed to find k_s. By measuring the pressure drop over the 6-m long test section, Eq. (13) could be used to determine k_s. For the present experiment, $k_s = 0.000163$ m; Olson & Eckert 1966 and Su & Gudmunsson 1998 found respectively 0.000132 and 0.000049 m.

Figure 3 compares Eq. (14) with the data of Olson & Eckert 1966 for several transpiration rates and measuring positions. The measurements of Olson & Eckert 1966 show a decrease in friction coefficient with an increase in the transpiration rate as expected. However, their data also show an increase in λ with an increase in the local Reynolds number. This has not been observed in the classical experiments of Nikuradse, for example. The predictions of Eq. (14), however, are coherent with the expected trends.

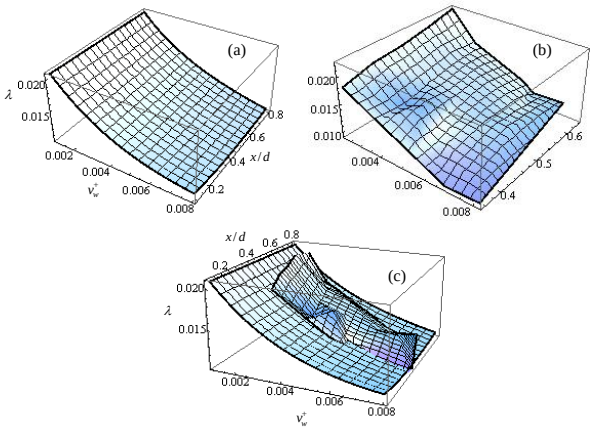

Figure 3. Friction coefficient for transpired flow over rough walls. a: present theory, b: data of Olson & Eckert 1966, c: comparison of (a) and (b).

The pressure drop due to frictional losses for the experimental conditions of Su & Gudmunsson 1998 are shown in Table 2. Note that results are presented for three distinct total flow rate ratio and Reynolds number. To all considered R_e, the theoretical predictions are very good for $\sigma =$ 0.02 and 0.05. In fact, in these ranges, the maximum prediction error is about 5%. For the highest σ (= 0.1), the error increases to 18%. Thus, the overall agreement of the present theory with the data of Su & Gudmunsson 1998 is surprisingly good. We have previously commented that the wall boundary condition for their experimental arrangement is not likely to approach a uniform condition.

Table 2. Predictions given by Eq. (14) as compared with the data of Su & Gudmunsson 1998.
σ = total flow rate ratio. Δp (Pa) = pressure loss.

R_e	σ	Δp *(Pa) Exp.*	Δp *(Pa) Th.*
40,000	0.02	1000	958
40,000	0.05	950	890
40,000	0.1	900	788
65,000	0.02	2450	2323
65,000	0.05	2350	2131
65,000	0.01	2250	1845
90,000	0.02	4900	4653
90,000	0.05	4700	4250
90,000	0.1	4500	3638

The performance of Eq. (14) against the present experimental data is shown in Table 3.

Table 3. Present work, Eq. (14).

R_e	Δp *(Pa) Exp.*	Δp *(Pa) Th.*
15,510	435	525
31,089	1795	1880
47,601	4050	4378

4.2. Two-phase flow

The first observable effect of flow transpiration on the general configuration of the slug flow was the break up of the of very elongated bubbles for conditions – as compared with the no-transpiration cases – in which the fluid and gas flow rates were about the same.

Mean velocity profiles for the liquid phase at station $x = 6$ m for two injection rates ($v_w^+ = v_w/U_{max}$) are shown in Figure 4(a). For a same injection velocity, the single- and two-phase velocity profiles shown in Figure 4(a) correspond to flows with about the same top centerline velocity. The presence of the gas phase makes the liquid velocity profiles less full as expected. The injection of fluid through the wall clearly modifies the velocity distribution, reducing the wall shear stress.

The streamwise velocity fluctuations are shown in Figure 4(b). The presence of bubbles in the flow naturally increases its degree of agitation, with a corresponding increase in $\sigma_u = \sqrt{\overline{u'^2}}$. The striking feature of Figure 4(b), however, is the large increase in σ_u due to the fluid transpiration at the wall. For the highest injection rate, $v_w^+ = 0.008$, a peak value of 0.4 ms^{-1} can be observed near the wall. The very pronounced level of turbulence near the wall might explain the break up of the very large bubbles.

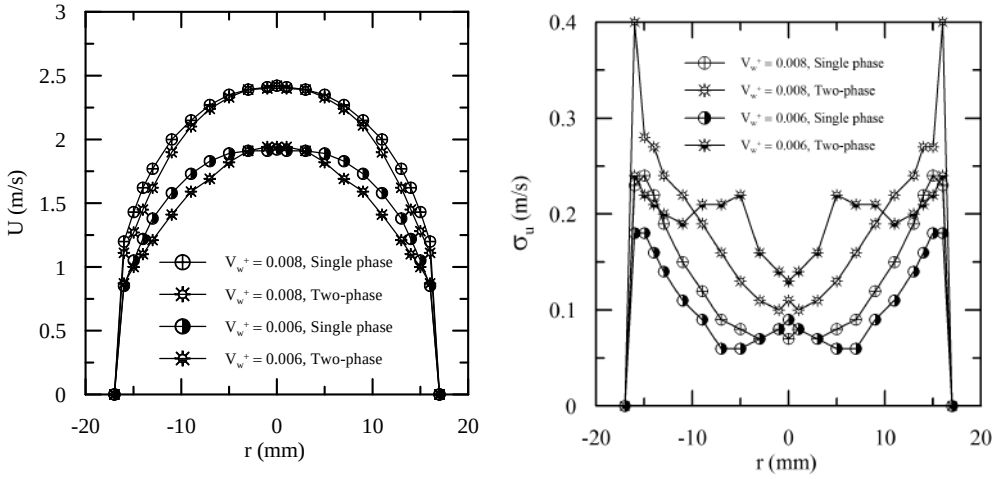

Figure 4. (a) Mean velocity profiles at station $x = 6$ m for the single and two-phase flow conditions with and without flow transpiration. (b) Streamwise velocity fluctuations $\sigma_u = \sqrt{\overline{u'^2}}$ at station $x = 6$ m for the single and two-phase flow conditions with and without flow transpiration .

The pressure drop distributions along the test section for several entrance Reynolds number (R_e) are shown in Figure 5(a) (single phase). An increase in R_e increases the pressure drop as expected. All results shown in Figure 5 agree with predictions given by Eq. (14).

Pressure drop distributions along the test section corresponding to the four exit velocity profiles shown in Figure 4(a) are shown in Figure 5(b). The less steep slopes of the two-phase flow velocity profiles result in a lesser pressure drop.

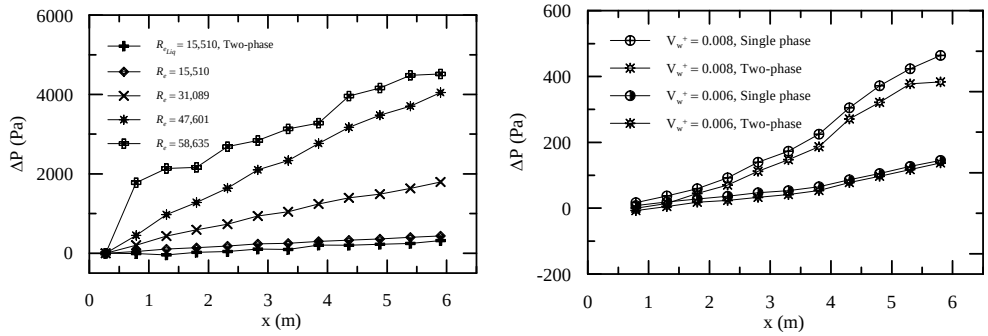

Figure 5. (a) Pressure drop distribution along test section. Flow conditions as in Table 1, five first entries. (b) Pressure drop distribution along test section. Flow conditions as in Table 1, last four entries.

5. Conclusion

The present work has studied the behaviour of slug flows in horizontal pipes with fluid injection at the wall. Nine different flow conditions have been scrutinized through measurements of pressure drop, local velocity and turbulence profiles.

The transpiration was observed to promote the formation of very large bubbles and the increase of near wall turbulence. These combined effects resulted in a decrease in pressure drop along the pipe.

Acknowledgments

Acknowledgments JBRL benefited from a CNPq Research Fellowship (Grant No 301172/2010-2). JBRL is also thankful to the Brazilian National Research Council (CNPq) for the financial support to this research through Grant 475759/2009-5. APSF is grateful to the Brazilian National Research Council (CNPq) for the award of a Research Fellowship (Grant No 303982/2009-8). The work was financially supported by CNPq through Grants No 473588/2009-9 and by the Rio de Janeiro Research Foundation (FAPERJ) through Grant E-26/170.005/2008.

References

[1] Berman, A. S. 1953 Laminar flow in channels with porous walls. *J. Appl. Physics* **24** 1323–1235.

[2] Bundy, D. & Weissberg, H. L. 1970 Experimental study of fully developed laminar flow in a porous pipe with wall injection. *Phys. Fluids* **13**, 2613–2615.

[3] Clemo, T. 2006 Flow in perforated pipes: a comparison of models and experiments. *SPE Production and Operations* **21**, 302–311.

[4] Cruz, M. D. G., Sousa, F. B. C. C., Rodrigues, D. ., Loureiro, J. B. R. & Silva Freire, A. P. 2009 Effects of flow transpiration on pressure losses in duct flow. *Brazilian Congress of Mechanical Engineering* , Porto Alegre, RS, Brazil.

[5] Erdogan, M. E. & Imrak, C. E. 2005 On the axial flow of an incompressible viscous fluid in a pipe with a porous boundary. *Acta Mechanica* **178** 187–197.

[6] Ligrani, P. M. & Moffat, R. J. 1986 Structure of transitionally rough and fully rough turbulent boundary layers. *J. Fluid Mech.* **162** 69–98.

[7] Nikuradse, J. 1933 Forschungsheft **301**.

[8] Olson, R. & Eckert, E. 1966 Experimental studies of turbulent flow in a porous circular tube with uniform fluid injection through the tube wall. *J. of Applied Mech.* **33** 7–17.

[9] Oxarango, L., Schmitz, P. & Quintard, M. 2004 Laminar flow in channels with wall suction or injection: a new model to study multi-channel filtration systems. *Chem. Eng. Sci.* **59** 1039–1057.

[10] Silva Freire, A. P. 1988 An asymptotic solution for transpired incompressible turbulent boundary layers. *Int. J. Heat Mass Transfer* **31** 1011–1021.

[11] Simpson, R. L. 1967 The turbulent boundary layer on a porous plate: an experimental study of the fluid dynamics with injection and suction. *Ph.D. thesis*, Stanford Univ., Stanford, California.

[12] Stevenson, T. N. 1963 A law of the wall for turbulent boundary layers with suction or injection. *Cranfield Rep. Aero.* **166**, The College of Aeronautics, Cranfield, England, U.K.

[13] Su, Z. & Gudmunsson, J. 1998 Perforation inflow reduces frictional pressure loss in horizontal wellbores. *J. Petroleum Sci. Eng.* **19** 223–232.

[14] Terrill, R. M. 1964 Laminar flow in a uniformly porous channel. *Aeronaut. Q.* **15** 299–310.